Progress In Electromagnetics Research, PIER 33, 219–235, 2001

ANALYTICAL ASYMPTOTIC EXTRACTION TECHNIQUE FOR THE ANALYSIS OF BEND DISCONTINUITY

C.-B. Chae, J.-P. Lee, and S.-O. Park

School of Electronics Engineering
Information and Communications University
58-4 Hwaam-dong, Yusung-gu
Taejon, 305-732, South Korea

K.-W. Suh

Department of Electronics Engineering
Kangnam University
San 6-2 Kugal-Ri, Yongin, 449-702, South Korea

Abstract—The purpose of this paper is to use the analytical asymptotic extraction technique to analyze the bend discontinuity. We show that the derived analytical techniques significantly reduce the computational time while improving the accuracy compared to the conventional method. Especially, the advantage of the proposed method can eliminate the truncation error for evaluating the asymptotic part of impedance matrix. The proposed method has applied for solving the bend discontinuity, and verified with measurement results.

1. INTRODUCTION

The conventional spectral domain method is too time-consuming to fill the impedance matrix elements because the matrix elements are expressed in terms of infinite double integrals and their integrands exhibit slow convergence and highly oscillating behavior. In the previous research of gap discontinuities, the analytical transformation of the infinite double integral into a finite one-dimensional integral in calculating the asymptotic impedance matrix elements had successfully in ref. [1]. This showed the dramatic improvement of the computation time for evaluating the overall impedance matrix elements without sacrificing the accuracy. With extension of the previous work, this paper presents efficient computational techniques in case of right-angled bend discontinuity. In order to describe the unknown current distributions, two kinds of expansion functions are used. The matrix element evaluations of the interactions between rooftop and half rooftop basis functions require extensive computation time. To overcome this computation time, we developed new analytical formulas for evaluating the asymptotic impedance matrix by using the above integral transform method. We show that the derived analytical techniques significantly reduce the computational time and improve the accuracy over the conventional method to evaluate the asymptotic part of impedance matrix by eliminating the truncation error for solving right-angled bend discontinuity. To validate this new approach, the results of commercial software and measurement are compared with those of the proposed method.

2. FORMULATION OF THE PROBLEM

The geometry of the bend discontinuity with a substrate is shown in Fig. 1. The substrate has a thickness of d and a relative permittivity of ϵ_r. The substrate and ground plane are assumed to be infinitely wide in the horizontal plane, and the conductors are assumed to be lossless and infinitesimally thin.

In order to apply the moment method, we define the dyadic Green's function due to infinitesimal current source on a grounded dielectric slab, which takes the form of [2, 3]

$$\tilde{G}_{xx}(k_x, k_y) = -j\frac{Z_0}{k_0}\frac{(\epsilon_r k_0^2 - k_x^2)k_2 + jk_1(k_0^2 - k_x^2)\tan(k_1 d)}{T_e T_m}\tan(k_1 d) \quad (1)$$

$$\tilde{G}_{yy}(k_x, k_y) = -j\frac{Z_0}{k_0}\frac{(\epsilon_r k_0^2 - k_y^2)k_2 + jk_1(k_0^2 - k_y^2)\tan(k_1 d)}{T_e T_m}\tan(k_1 d) \quad (2)$$

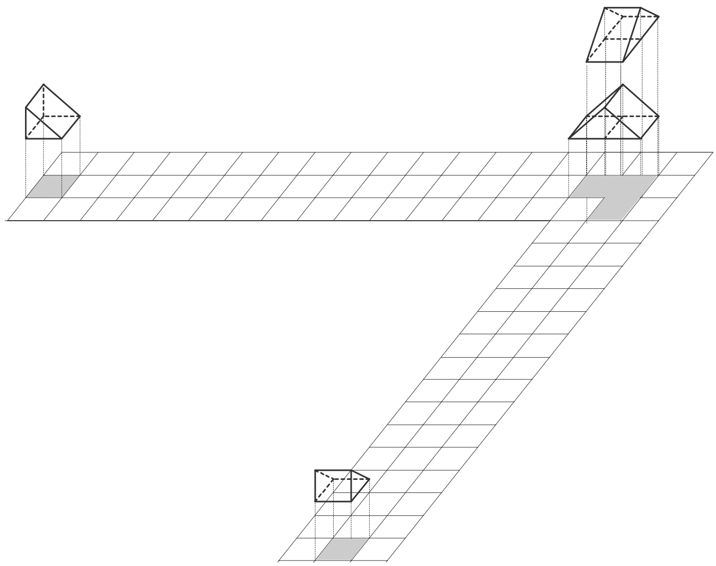

Figure 1. The geometry of a right-angle bend discontinuity.

$$\tilde{G}_{xy}(k_x, k_y) = \tilde{G}_{yx}(k_x, k_y) = -j\frac{Z_0}{k_0}\frac{k_x k_y \tan(k_1 d)[k_2 + jk_1 \tan(k_1 d)]}{T_e T_m} \quad (3)$$

where

$$\begin{aligned} T_e &= k_1 + jk_2 \tan(k_1 d) \\ T_m &= \epsilon_r k_2 + jk_1 \tan(k_1 d) \\ k_1^2 &= \epsilon_r k_0^2 - k_x^2 - k_y^2, \quad \mathrm{Im}\{k_1\} \leq 0 \\ k_2^2 &= k_0^2 - k_x^2 - k_y^2, \quad \mathrm{Im}\{k_2\} \leq 0 \\ \beta &= \sqrt{k_x^2 + k_y^2} \end{aligned} \quad (4)$$

and $k_0 = \omega\sqrt{\mu_0 \epsilon_0}$ where ω is the angular frequency, μ_0 and ϵ_0 are the permeability and permittivity of free-space, respectively.

The subscripts xy in $\tilde{G}_{xy}(k_x, k_y)$ represent an $\hat{x}$-directed electric field due to an infinitesimal $\hat{y}$-directed current source. The subscripts of the other Green's functions have similar designations. The respective asymptotic Green's functions of eqs. (1)–(3), for large β are given by

$$\tilde{G}_{xx}^{\infty}(k_x, k_y) = -j\frac{Z_0}{k_0}\left\{\frac{k_0^2}{2\beta} - \frac{k_x^2}{(\epsilon_r + 1)\beta}\right\} \quad (5)$$

$$\tilde{G}_{yy}^{\infty}(k_x,k_y) = -j\frac{Z_0}{k_0}\left\{\frac{k_0^2}{2\beta}-\frac{k_y^2}{(\epsilon_r+1)\beta}\right\} \tag{6}$$

$$\tilde{G}_{xy}^{\infty}(k_x,k_y) = \tilde{G}_{yx}^{\infty}(k_x,k_y) = j\frac{Z_0}{k_0}\frac{k_xk_y}{(\epsilon_r+1)\beta} \tag{7}$$

To solve for the surface current density on the patch using moment method, the next step is to express the surface current density as a linear combination of the basis functions, which are chosen in this work to be roof-top and half roof-top. A set of roof-top functions are employed to model the current density distribution on the conductor. The current densities at the load terminals are modeled by a half roof-top basis functions. The current densities can be expressed as

$$J_{mn}^x(x,y) = \left(1-\frac{|x-x_m|}{\Delta x}\right)\cdot \mathrm{rect}\left(\frac{y-y_n}{\Delta y}\right), \quad \frac{|x-x_m|}{\Delta x}<1, \frac{|y-y_n|}{\Delta y}<\frac{1}{2} \tag{8}$$

$$J_{mn}^y(x,y) = \mathrm{rect}\left(\frac{y-y_n}{\Delta y}\right)\cdot\left(1-\frac{|x-x_m|}{\Delta x}\right), \quad \frac{|x-x_m|}{\Delta x}<\frac{1}{2}, \frac{|y-y_n|}{\Delta y}<1 \tag{9}$$

$$J_{Load}^x(x,y) = \left(1-\frac{x}{\Delta x}\right)\cdot \mathrm{rect}\left(\frac{y-y_n}{\Delta y}\right), \quad \frac{|x|}{\Delta x}<1, \frac{|y-y_n|}{\Delta y}<\frac{1}{2} \tag{10}$$

$$J_{Load}^y(x,y) = \mathrm{rect}\left(\frac{y-y_n}{\Delta y}\right)\cdot\left(1-\frac{x}{\Delta x}\right), \quad \frac{|x-x_m|}{\Delta x}<\frac{1}{2}, \frac{|y|}{\Delta y}<1 \tag{11}$$

where

$$\mathrm{rect}\left(\frac{x}{L}\right) = \begin{cases}1, & |x|<L/2\\ 0, & |x|>L/2.\end{cases} \tag{12}$$

The fourier transforms of the $\hat{x}$-directed roof-top and half roof-top current density of eq.(8) and eq.(10) can be expressed as

$$\tilde{J}_{mn}^x(k_x,k_y) = \frac{8}{\Delta x}\cdot\frac{\sin^2(k_x\frac{\Delta x}{2})}{k_x^2}\cdot\frac{\sin(k_y\frac{\Delta y}{2})}{k_y}\cdot e^{-j(k_xx_m+k_yy_n)} \tag{13}$$

$$\tilde{J}_{Load}^x(k_x,k_y) = \frac{2}{\Delta x}\cdot\frac{2\sin^2(k_x\frac{\Delta x}{2})-j\Delta xk_x+j\sin k_x\Delta x}{k_x^2}\cdot\frac{\sin(k_y\frac{\Delta y}{2})}{k_y}\cdot e^{-j(k_xx_0+k_yy_n)} \tag{14}$$

Using Galerkin's method, and employing the asymptotic extraction technique, impedance matrix can be expressed as

$$\overline{\overline{Z}}_{mnm'n'} =$$
$$-\frac{1}{4\pi^2}\int_{\infty}^{\infty}\int_{\infty}^{\infty}\vec{\tilde{J}}_{mn}(k_x,k_y)\left[\overline{\overline{\tilde{G}}}(k_x,k_y)-\overline{\overline{\tilde{G}}}^{\infty}(k_x,k_y)\right]\vec{\tilde{J}}^{*}_{m'n'}(k_x,k_y)dk_xdk_y$$
$$-\frac{1}{4\pi^2}\int_{\infty}^{\infty}\int_{\infty}^{\infty}\vec{\tilde{J}}_{mn}(k_x,k_y)\overline{\overline{\tilde{G}}}^{\infty}(k_x,k_y)\vec{\tilde{J}}^{*}_{m'n'}(k_x,k_y)dk_xdk_y \quad (15)$$

$$\overline{\overline{Z}}_{Load,mn} =$$
$$-\frac{1}{4\pi^2}\int_{\infty}^{\infty}\int_{\infty}^{\infty}\vec{\tilde{J}}_{Load}(k_x,k_y)\left[\overline{\overline{\tilde{G}}}(k_x,k_y)-\overline{\overline{\tilde{G}}}^{\infty}(k_x,k_y)\right]\vec{\tilde{J}}^{*}_{mn}(k_x,k_y)dk_xdk_y$$
$$-\frac{1}{4\pi^2}\int_{\infty}^{\infty}\int_{\infty}^{\infty}\vec{\tilde{J}}_{Load}(k_x,k_y)\overline{\overline{\tilde{G}}}^{\infty}(k_x,k_y)\vec{\tilde{J}}^{*}_{mn}(k_x,k_y)dk_xdk_y \quad (16)$$

The first double integral in eqs. (15) and (16) converges more rapidly to zero than the double integral of original form. The integrand of the second infinite double integral in eqs. (15) and (16) exhibits slowly convergent and highly oscillatory behavior, which leads to difficulties when attempting to evaluate it using a direct numerical integration. Therefore, the main objective of this paper is to solve the second integral in eqs. (15) and (16) by an analytical technique.

3. EVALUATION OF ASYMPTOTIC IMPEDANCE MATRIX

The asymptotic impedance matrix of the second integral in eq. (15) and (16), associating with the roof-top, half roof-top functions of eq. (13) and (14) and the asymptotic Green's function of eq. (1)–(3), can be expressed as

$$Z^{xx^{Asy}}_{mnm'n'} = -\frac{j}{\pi^2}\frac{Z_0}{k_0}\left(\frac{8}{\Delta x}\right)^2\left\{-\frac{k_0^2}{2}I^{xx^a}_{mnm'n'}+\frac{1}{(\epsilon_r+1)}I^{xx^b}_{mnm'n'}\right\} \quad (17)$$

$$Z^{xy^{Asy}}_{mnm'n'} = \frac{j}{\pi^2}\frac{Z_0}{k_0}\left(\frac{64}{\Delta x\cdot\Delta y}\right)\frac{1}{(\epsilon_r+1)}I^{xy}_{mnm'n'} \quad (18)$$

$$Z^{xx^{Asy}}_{Load,mn} = -\frac{j}{\pi^2}\frac{Z_0}{k_0}\left(\frac{4}{\Delta x}\right)^2\left\{-\frac{k_0^2}{2}I^{xx^a}_{Load,mn}+\frac{1}{(\epsilon_r+1)}I^{xx^b}_{Load,mn}\right\} \quad (19)$$

$$Z^{xy^{Asy}}_{Load,mn} = \frac{j}{\pi^2}\frac{Z_0}{k_0}\left(\frac{16}{\Delta x\cdot\Delta y}\right)\frac{1}{(\epsilon_r+1)}I^{xy}_{Load,mn} \quad (20)$$

with

$$I^{xx^a}_{mnm'n'} = \int_0^\infty \int_0^\infty \frac{\cos(k_x x_s)}{\sqrt{k_x^2+k_y^2}} \frac{\sin^2(k_y \frac{\Delta y}{2})}{k_y^2} \frac{\sin^4(k_x \frac{\Delta x}{2})}{k_x^4} \cos(k_y y_s) dk_x dk_y \tag{21}$$

$$I^{xx^b}_{mnm'n'} = \int_0^\infty \int_0^\infty \frac{\cos(k_x x_s)}{\sqrt{k_x^2+k_y^2}} \frac{\sin^2(k_y \frac{\Delta y}{2})}{k_y^2} \frac{\sin^4(k_x \frac{\Delta x}{2})}{k_x^2} \cos(k_y y_s) dk_x dk_y \tag{22}$$

$$I^{xy}_{mnm'n'} = -\int_0^\infty \int_0^\infty \frac{\sin(k_x x_s)}{\sqrt{k_x^2+k_y^2}} \frac{\sin^3(k_y \frac{\Delta y}{2})}{k_x^2} \frac{\sin^3(k_x \frac{\Delta x}{2})}{k_y^2} \sin(k_y y_s) dk_x dk_y \tag{23}$$

$$\begin{aligned} I^{xx^a}_{Load,mn} = {} & 2\int_0^\infty \int_0^\infty \frac{\cos(k_x x_s)}{\sqrt{k_x^2+k_y^2}} \frac{\sin^2(k_y \frac{\Delta y}{2})}{k_y^2} \frac{\sin^4(k_x \frac{\Delta x}{2})}{k_x^4} \cos(k_y y_s) dk_x dk_y \\ & + \int_0^\infty \int_0^\infty \frac{1}{\sqrt{k_x^2+k_y^2}} \frac{\sin^2(k_y \frac{\Delta y}{2})}{k_y^2} \frac{\sin^2(k_x \frac{\Delta x}{2})}{k_x^4} \\ & \times \{k_x \sin(k_x x_s)\Delta x - \sin(k_x \Delta x)\sin(k_x x_s)\} \cos(k_y y_s) dk_x dk_y \end{aligned} \tag{24}$$

$$\begin{aligned} I^{xx^b}_{Load,mn} = {} & 2\int_0^\infty \int_0^\infty \frac{\cos(k_x x_s)}{\sqrt{k_x^2+k_y^2}} \frac{\sin^2(k_y \frac{\Delta y}{2})}{k_y^2} \frac{\sin^4(k_x \frac{\Delta x}{2})}{k_x^2} \cos(k_y y_s) dk_x dk_y \\ & + \int_0^\infty \int_0^\infty \frac{1}{\sqrt{k_x^2+k_y^2}} \frac{\sin^2(k_y \frac{\Delta y}{2})}{k_y^2} \frac{\sin^2(k_x \frac{\Delta x}{2})}{k_x^2} \\ & \times \{k_x \sin(k_x x_s)\Delta x - \sin(k_x \Delta x)\sin(k_x x_s)\} \cos(k_y y_s) dk_x dk_y \end{aligned} \tag{25}$$

$$\begin{aligned} I^{xy}_{Load,mn} = {} & -\int_0^\infty \int_0^\infty \frac{\cos(k_x x_s)}{\sqrt{k_x^2+k_y^2}} \frac{\sin(k_y \frac{\Delta y}{2})}{k_x^2} \frac{\sin^3(k_x \frac{\Delta x}{2})}{k_y^2} \\ & \times \{\Delta x k_x \sin(k_y y_s) - \sin(k_x \Delta x)\sin(k_y y_s)\} dk_x dk_y \\ & + 2\int_0^\infty \int_0^\infty \frac{\sin(k_x x_s)}{\sqrt{k_x^2+k_y^2}} \frac{\sin^3(k_x \frac{\Delta x}{2})}{k_x^2} \frac{\sin^3(k_y \frac{\Delta y}{2})}{k_y^2} \sin(k_y y_s) dk_x dk_y \end{aligned} \tag{26}$$

where the even and odd properties of the integrand are used to reduce the integration range in eqs. (21)–(26).

Equations (21)–(23) already had solved in analytical solution in ref. [1]. Thus this paper shows an analytic solution for eqs. (24)–(26). Each integrand in eqs. (24)–(26) is not separable in terms of k_x and k_y due to the $1/\sqrt{k_x^2+k_y^2}$ term, which prevents it from being reduced to the product of two one-dimensional integrals. By introducing the same technique represented by [4, eq. (11)], the integrals of eqs. (24)–(26) can be expressed as

$$\begin{aligned}
I^{xx^a}_{Load,mn} = {} & \frac{2}{\pi}\int_{-\infty}^{\infty}\left\{\int_0^{\infty} K_0(k_y|\chi - x_s|)\frac{\sin^2(k_y\frac{\Delta y}{2})}{k_y^2}\cos(k_y y_s)dk_y\right.\\
&\left.\times\int_0^{\infty}\frac{\sin^4(k_x\frac{\Delta x}{2})}{k_x^4}\cos(k_x\chi)dk_x\right\}d\chi\\
&+\frac{1}{\pi}\int_{-\infty}^{\infty}\left\{\int_0^{\infty} K_0(k_y|\chi - x_s|)\frac{\sin^2(k_y\frac{\Delta y}{2})}{k_y^2}\cos(k_y y_s)dk_y\right.\\
&\left.\times\int_0^{\infty}\frac{\Delta x\sin^2(k_x\frac{\Delta x}{2})}{k_x^3}\sin(k_x x_s)\cos(k_x\chi)dk_x\right\}d\chi\\
&-\frac{1}{\pi}\int_{-\infty}^{\infty}\left\{\int_0^{\infty} K_0(k_y|\chi - x_s|)\frac{\sin^2(k_y\frac{\Delta y}{2})}{k_y^2}\cos(k_y y_s)dk_y\right.\\
&\left.\times\int_0^{\infty}\frac{\sin^2(k_x\frac{\Delta x}{2})\sin(k_x\Delta x)}{k_x^4}\sin(k_x x_s)\cos(k_x\chi)dk_x\right\}d\chi
\end{aligned}\tag{27}$$

$$\begin{aligned}
I^{xx^b}_{Load,mn} = {} & \frac{2}{\pi}\int_{-\infty}^{\infty}\left\{\int_0^{\infty} K_0(k_y|\chi - x_s|)\frac{\sin^2(k_y\frac{\Delta y}{2})}{k_y^2}\cos(k_y y_s)dk_y\right.\\
&\left.\times\int_0^{\infty}\frac{\sin^4(k_x\frac{\Delta x}{2})}{k_x^2}\cos(k_x\chi)dk_x\right\}d\chi\\
&+\frac{1}{\pi}\int_{-\infty}^{\infty}\left\{\int_0^{\infty} K_0(k_y|\chi - x_s|)\frac{\sin^2(k_y\frac{\Delta y}{2})}{k_y^2}\cos(k_y y_s)dk_y\right.\\
&\left.\times\int_0^{\infty}\frac{\Delta x\sin^2(k_x\frac{\Delta x}{2})}{k_x}\sin(k_x x_s)\cos(k_x\chi)\right\}d\chi\\
&-\frac{1}{\pi}\int_{-\infty}^{\infty}\left\{\int_0^{\infty} K_0(k_y|\chi - x_s|)\frac{\sin^2(k_y\frac{\Delta y}{2})}{k_y^2}\cos(k_y y_s)dk_y\right.\\
&\left.\times\int_0^{\infty}\frac{\sin^2(k_x\frac{\Delta x}{2})\sin(k_x\Delta x)}{k_x^2}\sin(k_x x_s)\cos(k_x\chi)\right\}d\chi
\end{aligned}\tag{28}$$

$$\begin{aligned}
I^{xy}_{Load,mn} = & -\frac{1}{\pi}\int_{\infty}^{\infty}\left\{\int_0^{\infty} K_0(k_y|\chi-x_s|)\frac{\sin^3(k_y\frac{\Delta y}{2})}{k_y^2}\sin(k_y y_s)dk_y \right.\\
& \left.\times\int_0^{\infty}\frac{\Delta x\sin(k_x\frac{\Delta x}{2})}{k_x}\cos(k_x\chi)dk_x\right\}d\chi \\
& -\frac{1}{\pi}\int_{\infty}^{\infty}\left\{\int_0^{\infty} K_0(k_y|\chi-x_s|)\frac{\sin^3(k_y\frac{\Delta y}{2})}{k_y^2}\sin(k_y y_s)dk_y \right.\\
& \left.\times\int_0^{\infty}\frac{\Delta x\sin(k_x\frac{\Delta x}{2})\sin(k_x\Delta x)}{k_x^2}\cos(k_x\chi)dk_x\right\}d\chi \\
& -\frac{2}{\pi}\int_{-\infty}^{\infty}\left\{\int_0^{\infty} K_0(k_y\chi)\frac{\sin^3(k_y\frac{\Delta y}{2})}{k_y^2}\sin(k_y y_s)dk_y \right.\\
& \left.\times\int_0^{\infty}\frac{\sin^3(k_x\frac{\Delta x}{2})}{k_x^2}\sin(k_x x_s)\cos(k_x\chi)dk_x\right\}d\chi \qquad (29)
\end{aligned}$$

where K_0 is the modified Bessel function of the first kind.

The infinite six-fold integrals of eqs. (27)–(29) can be converted into three 1-D integrals if the separate integrals with respect to k_x and k_y can be evaluated in closed form. To accomplish this, the first integrals in eqs. (27)–(29) with respect to k_y are defined as

$$\mathcal{A}(\chi-x_s) = \int_0^{\infty} K_0(k_y|\chi-x_s|)\frac{\sin^2(k_y\frac{\Delta y}{2})}{k_y^2}\cos(k_y y_s)dk_y \qquad (30)$$

$$\mathcal{B}(\chi) = \int_0^{\infty} K_0(k_y\chi)\frac{\sin^3(k_y\frac{\Delta y}{2})}{k_y^2}\sin(k_y y_s)dk_y \qquad (31)$$

where $\mathcal{A}(\chi-x_s)$ and $\mathcal{B}(\chi)$ can be solved analytically. Their detailed derivations are presented in ref. [1].

The second integrals in eqs. (27) and (28), with respect to k_x, were derived in [1] and integral is expressed as

$$\begin{aligned}
\mathcal{S}_a(\chi) &= \int_0^{\infty}\frac{\sin^4(k_x\frac{\Delta x}{2})}{k_x^4}\cos(k_x\chi)dk_x \\
&= \begin{cases} \frac{\pi}{96}\{(2\Delta x-|\chi|)^3-4(\Delta x-|\chi|)^3\}, & |\chi|<\Delta x \\ \frac{\pi}{96}(2\Delta x-|\chi|)^3, & \Delta x\le|\chi|<2\Delta x \\ 0, & \text{otherwise}\end{cases} \qquad (32)
\end{aligned}$$

$$\mathcal{S}_d(\chi) = \int_0^{\infty}\frac{\sin^4(k_x\frac{\Delta x}{2})}{k_x^2}\cos(k_x\chi)dk_x$$

$$= \begin{cases} \frac{\pi}{2}(\frac{1}{4}\Delta x - \frac{3}{8}\chi), & |\chi| < \Delta x \\ \frac{\pi}{2}(-\frac{1}{4}\Delta x + \frac{1}{8}\chi), & \Delta x \leq |\chi| < 2\Delta x \\ 0, & |\chi| \geq 2\Delta x \end{cases} \tag{33}$$

By using formula 3.828.5 and 3.828.15 of [5], we can get the following formulas to evaluate:

$$\begin{aligned} \mathcal{PS}_b(\chi) &= \int_0^\infty \frac{\sin^2(k_x \frac{\Delta x}{2})}{k_x^3} \sin(k_x \chi) dk_x \\ &= \begin{cases} \frac{\pi}{4}\Big(\Delta x|\chi| - \frac{\chi^2}{2}\Big), & |\chi| < \Delta x \\ 0, & \text{otherwise} \end{cases} \end{aligned} \tag{34}$$

$$\begin{aligned} \mathcal{PS}_c &= \int_0^\infty \frac{\sin^2(k_x \frac{\Delta x}{2}) \sin(k_x \Delta x)}{k_x^4} \sin(k_x \chi) dk_x \\ &= \begin{cases} -\frac{\pi}{16}(4\Delta x^2 - 2\Delta x \chi + \frac{1}{3}\chi^3), & -2\Delta x < \chi < -\frac{2}{3}\Delta x \\ \frac{\pi}{8}(\frac{2}{3}\Delta x^2 \chi - \frac{1}{3}\chi^3), & -\frac{2}{3}\Delta x < \chi < \frac{2}{3}\Delta x \\ \frac{\pi}{16}(4\Delta x^2 - 2\Delta x \chi + \frac{1}{3}\chi^3), & \frac{2}{3}\Delta x < \chi < 2\Delta x \\ 0, & \text{otherwise} \end{cases} \end{aligned} \tag{35}$$

With the aid of eq. (34), the fourth integral of eq. (27) with respect k_x is represented by

$$\begin{aligned} \mathcal{S}_b(\chi) &= \int_0^\infty \frac{\sin^2(k_x \frac{\Delta x}{2})}{k_x^3} \sin(k_x x_s) \cos(k_x \chi) dk_x \\ &= \frac{1}{2}[\mathcal{PS}_b(\chi + x_s) - \mathcal{PS}_b(\chi - x_s)] \end{aligned} \tag{36}$$

In this manner, the sixth integral of eq. (27) with respect k_x is represented by

$$\begin{aligned} \mathcal{S}_c(\chi) &= \int_0^\infty \frac{\sin^2(k_x \frac{\Delta x}{2}) \sin(k_x \Delta x)}{k_x^4} \sin(k_x x_s) \cos(k_x \chi) dk_x \\ &= \frac{1}{2}[\mathcal{PS}_c(\chi + x_s) - \mathcal{PS}_c(\chi - x_s)] \end{aligned} \tag{37}$$

With the aid of eq. (36) and eq. (37), eq. (27) is reduced to

$$\begin{aligned} I_{Load,mn}^{xx^a} &= \frac{2}{\pi} \int_{-2\Delta x}^{2\Delta x} \mathcal{A}(\chi - x_s) \cdot \mathcal{S}_a(\chi) d\chi \\ &\quad + \frac{\Delta x}{\pi} \int_{-\Delta x + x_s}^{\Delta x + x_s} \mathcal{A}(\chi - x_s) \cdot \mathcal{PS}_b(\chi - x_s) d\chi \\ &\quad - \frac{1}{\pi} \int_{-2\Delta x + x_s}^{2\Delta x + x_s} \mathcal{A}(\chi - x_s) \cdot \mathcal{PS}_c(\chi - x_s) d\chi \end{aligned} \tag{38}$$

where the even property of $\mathcal{A}(\chi)$ is used to reduce the two integrals to one integral.

In the same way of eq. (27), we can get the analytical formula of eq. (28). By using formula 3.828.3 and 3.828.13.2 of [5], it can be written as

$$\mathcal{PS}_e(\chi) = \int_0^\infty \frac{\sin^2(k_x\frac{\Delta x}{2})}{k_x}\sin(k_x\chi)dk_x = \frac{\pi}{4}\mathrm{rect}\Big(\frac{\chi}{2\Delta x}\Big) \tag{39}$$

$$\begin{aligned}\mathcal{PS}_f(\chi) &= \int_0^\infty \frac{\sin^2(k_x\frac{\Delta x}{2})\sin(k_x\Delta x)}{k_x^2}\sin(k_x\chi)dk_x \\ &= \begin{cases} \frac{\pi}{8}(\chi), & -2\Delta x < \chi < -\frac{2}{3}\Delta x \\ \frac{\pi}{4}(\chi), & -\frac{2}{3}\Delta x < \chi < \frac{2}{3}\Delta x \\ -\frac{\pi}{8}(\chi), & \frac{2}{3}\Delta x < \chi < 2\Delta x \\ 0, & \text{otherwise}\end{cases}\end{aligned} \tag{40}$$

With aid of eq. (39), eq. (40), the fourth and sixth integrals of eq. (28) with respect to k_x are represented by

$$\begin{aligned}\mathcal{S}_e(\chi) &= \int_0^\infty \frac{\sin^2(k_x\frac{\Delta x}{2})}{k_x}\sin(k_x x_s)\cos(k_x\chi)dk_x \\ &= \frac{1}{2}[\mathcal{PS}_{e1}(\chi+x_s) - \mathcal{PS}_{e1}(\chi-x_s)]\end{aligned} \tag{41}$$

$$\begin{aligned}\mathcal{S}_f(\chi) &= \int_0^\infty \frac{\sin^2(k_x\frac{\Delta x}{2})\sin(k_x\Delta x)}{k_x^2}\sin(k_x x_s)\cos(k_x\chi)dk_x \\ &= \frac{1}{2}[\mathcal{PS}_{e2}(\chi+x_s) - \mathcal{PS}_{e2}(\chi-x_s)]\end{aligned} \tag{42}$$

With the aid of eq. (41) and eq. (42), eq. (28) is reduced to

$$\begin{aligned}I^{xx^b}_{Load,mn} &= \frac{2}{\pi}\int_{-2\Delta x}^{2\Delta x}\mathcal{A}(\chi-x_s)\cdot\mathcal{S}_d(\chi)d\chi \\ &\quad+\frac{\Delta x}{\pi}\int_{-\Delta x+x_s}^{\Delta x+x_s}\mathcal{A}(\chi-x_s)\cdot\mathcal{PS}_e(\chi-x_s)d\chi \\ &\quad-\frac{1}{\pi}\int_{-2\Delta x+x_s}^{2\Delta x+x_s}\mathcal{A}(\chi-x_s)\cdot\mathcal{PS}_f(\chi-x_s)d\chi\end{aligned} \tag{43}$$

The second and fourth integrals in eq. (29), with respect to k_x, were derived in Appendix A, and written as follows;

$$\mathcal{S}_g(\chi) = \int_0^\infty \frac{\sin(k_x\frac{\Delta x}{2})}{k_x}\cos(k_x\chi)dk_x = \begin{cases}\frac{\pi}{2}, & |\chi| < \frac{\Delta x}{2} \\ 0, & |\chi| > \frac{\Delta x}{2}\end{cases} \tag{44}$$

$$\mathcal{S}_h(\chi) = \int_0^\infty \frac{\sin(k_x \frac{\Delta x}{2}) \sin(k_x \Delta x)}{k_x^2} \cos(k_x \chi) dk_x$$
$$= \begin{cases} \frac{\pi}{2}(\frac{\Delta x}{4}), & |\chi| < \frac{\Delta x}{2} \\ \frac{\pi}{2}(\frac{3}{8}\Delta x - \frac{1}{4}|\chi|), & \frac{\Delta x}{2} \le |\chi| < \frac{3\Delta x}{2} \\ 0, & \frac{3\Delta x}{2} < |\chi| \end{cases} \quad (45)$$

By taking the derivative with respect to b on both sides of [5], formula 3.828.15 with changing the parameters can be rewritten as;

$$\mathcal{PS}_i(\chi) = \int_0^\infty \frac{\sin^3(k_x \frac{\Delta x}{2})}{k_x^2} \sin(k_x \chi) dk_x$$
$$= \begin{cases} -\frac{\pi}{8}(\frac{3\Delta x}{2} + \chi), & -\frac{3\Delta x}{2} < \chi < -\frac{\Delta x}{2} \\ \frac{\pi}{4}(\chi), & -\frac{\Delta x}{2} < \chi < \frac{\Delta x}{2} \\ \frac{\pi}{8}(\frac{3\Delta x}{2} - \chi), & \frac{\Delta x}{2} < \chi < \frac{3\Delta x}{2} \\ 0, & \text{otherwise.} \end{cases} \quad (46)$$

With the aid of eq. (46), the sixth integral of eq. (29) with respect to k_x is represented by

$$\mathcal{S}_i(\chi) = \int_0^\infty \frac{\sin^3(k_x \frac{\Delta x}{2})}{k_x^2} \sin(k_x x_s) \cos(k_x \chi) dk_x$$
$$= \frac{1}{2}[\mathcal{PS}_i(\chi + x_s) - \mathcal{PS}_i(\chi - x_s)]. \quad (47)$$

Since $\mathcal{S}_g$, $\mathcal{S}_h$, and $\mathcal{PS}_i$ are compactly supported in the finite region, the infinite double integrals of eq. (29) can be converted into finite 1-D integrals as follows;

$$I^{xy}_{Load,mn} = -\frac{\Delta x}{\pi} \int_{-\frac{\Delta x}{2} - x_s}^{\frac{\Delta x}{2} - x_s} \mathcal{B}(\chi) \cdot \mathcal{S}_g(\chi + x_s) d\chi$$
$$-\frac{\Delta x}{\pi} \int_{-\frac{3\Delta x}{2} - x_s}^{\frac{3\Delta x}{2} - x_s} \mathcal{B}(\chi) \cdot \mathcal{S}_h(\chi + x_s) d\chi$$
$$+\frac{1}{\pi} \int_{-\frac{3\Delta x}{2} + x_s}^{\frac{3\Delta x}{2} + x_s} \mathcal{B}(\chi) \cdot \mathcal{PS}_i(\chi - x_s) d\chi \quad (48)$$

In order to verify, we make comparisons between the two methods (the finite 1-D integrals and the other using double infinite integrals) in terms of accuracy and execution time. As an example, the finite 1-D integrals of eq. (38) and eq. (43) are evaluated at the parameters $\Delta x = \Delta y = 1$ and $y_s = 0 \cdot \Delta y$ for $0 \le x_s \le 10$ and eq. (48)

evaluated at the parameters $\Delta x = \Delta y = 1$ and $y_s = 3 \cdot \Delta y/2$. With these parameters, the 2-D integrals of 27–29 are calculated with self-adaptive numerical quadratures with an upper truncation limit of β^u=300(rad/mm). The results are plotted in Fig. 2, which indicate excellent agreement with each other.

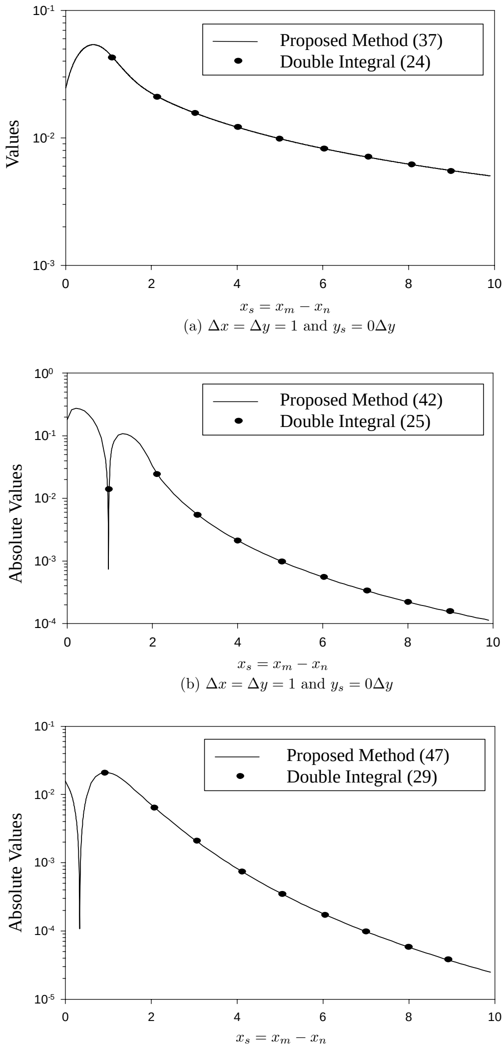

(a) $\Delta x = \Delta y = 1$ and $y_s = 0\Delta y$

(b) $\Delta x = \Delta y = 1$ and $y_s = 0\Delta y$

(c) $\Delta x = \Delta y = 1$ and $y_s = 3\Delta y/2$

Figure 2. Comparison between the infinite 2-D integral and the infinite 1-D integral of $I_{Load,mn}$.

4. NUMERICAL RESULTS

To verify the proposed method, computations were made and were compared with measurements and other available numerical data. The structure investigated is 2.4-mm strip width on a grounded dielectric substrate with thickness $d = 31\,\text{mil}$ and dielectric constant $\epsilon_r = 2.33$.

Enforcing the boundary condition on the surface of a perfectly conducting patch and applying the Galerkin's procedure, the matrix equations for the unknown coefficients of the basis functions can be obtained as

$$\begin{bmatrix} Z^{xx}_{mnm'n'} & Z^{xy}_{mnm'n'} \\ Z^{yx}_{mnm'n'} & Z^{yy}_{mnm'n'} \end{bmatrix} \begin{bmatrix} I^{x}_{m'n'} \\ I^{y}_{m'n'} \end{bmatrix} = \begin{bmatrix} V^{x}_{mn} \\ V^{y}_{mn} \end{bmatrix} \tag{49}$$

where $Z_{mnm'n'}$ denotes the mutual impedance between the (m, n)th testing function and the (m', n')th basis function, and V_{mn} represents the excitation voltage at the (m, n)th position of the element due to the current source.

Then we consider the evaluation of the matrix elements of eq. (49). The double infinite integral in each submatrix is carried out by the asymptotic extraction technique described in eq. (15) and (16). The first integrand of the first integral in eq. (15) and (16) is performed numerically, after transforming into polar coordinates. The integrand of the first double integral in eq. (15) and (16) possesses singularities corresponding to the surface wave poles. In this paper, these poles are evaluated with the use of a folding technique.

The second integral in eqs. (15) and (16) is computed directly from the transformed 1-D integral integration algorithm. The direct double integration of the second integral in eqs. (15) and (16) is the most time consuming part of the overall computation of the matrix elements. However, the calculation of this tail integral using the transformed finite 1-D integral has almost negligible computation time as compared to those of the first integral in eqs. (15) and (16).

The matrix equation in (49) can not be solved uniquely for the coefficients of the basis function unless additional equations, obtained by imposing the boundary conditions at the load terminals, are added. They relate the coefficients of the load basis functions to the remainder of the basis functions in terms of the complex load impedances. For example, the additional equation at the load terminal can be written as [6, 7]

$$\left(1 + j\beta\Delta x \frac{Z_L}{Z_0} - \frac{\beta^2 \Delta x^2}{2}\right) I_{-N-1} - I_{-N} = 0 \tag{50}$$

By using these additional equations in the matrix (49), one can solve the current distribution on the conductor.

The current distribution on the structure obtained from the above mentioned method is approximated by a sum of complex exponentials. In order to extract the scattering parameters, we employ the Matrix Pencil Method [8], and impose the constraint that the number of exponential terms representing the current distribution on the transmission line is only three, i.e., incident wave, reflected wave, and high order terms.

The s-parameters of a right-angled bend discontinuity is computed by using the above mentioned numerical techniques. Our results are compared with the measured data as well as those using Ensemble software. Their respective results are included in Fig. 3. For the results of the method of this paper and Ensemble data, there is a good agreement with each other over a wide range of frequencies.

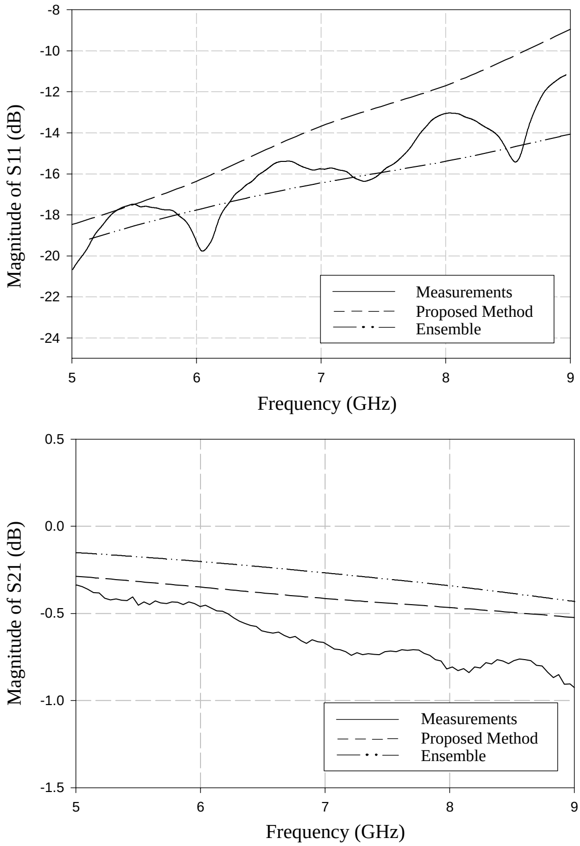

Figure 3. Comparison between measured and predicted S-parameters of bend discontinuity.

To illustrate the overall speed of the computation time, the CPU time between the proposed method and the conventional spectral domain method without acceleration to obtain the S-parameters is compared for a right-angled bend discontinuity at a single frequency of 5 GHz. In Table 1, the CPU times are given. Using the proposed method, the chosen upper limit of $50k_0$ to evaluate the integral of the matrix elements allows the result to be accurate more than conventional spectral domain method. However, the conventional spectral domain approach uses the upper limit of β^u reaches $500k_0$ which has the same accuracy level of the proposed method. As seen in Table 1, the overall computation time of the proposed method is 44.06 times faster than that of the conventional method. Also the accuracy of the proposed method is quite comparable with that of the conventional method.

Table 1. CPU time on a P-III 800 MHz (RAM 1 GB) PC for the analysis of bend discontinuity (strip width=2.4 mm, $\epsilon_r = 2.2$, $d = 31\,\text{mil}$, $f = 5\,\text{GHz}$).

SDA without acceleration(a) (seconds)	Proposed Method(b) (seconds)	Speed Improvement $\frac{a}{b}$
3473	78	44.06

5. CONCLUSION

Using the integral transform technique, the infinite double integral in the evaluation of the asymptotic part of the impedance matrix with roof-top and half roof-top basis functions was reduced to a finite one-dimensional integral. This method was applied to the right-angel bend discontinuity. The computed results were compared with those of other methods and measured data. It is shown that the proposed method significantly reduces the computational effort while retaining its accuracy. These features give room for future application to an accurate and efficient CAD tool that handles arbitrarily shaped planar circuits.

APPENDIX A. SOLUTIONS OF INTEGRAL EQ. (45)

The integral $\mathcal{S}_h$ in eq. (45) over the k_x plane can be converted into an integration over the x plane by using Parseval's theorem

$$\begin{aligned}\mathcal{S}_h(\chi) &= \int_0^\infty \frac{\sin(k_x\frac{\Delta x}{2})\sin(k_x\Delta x)}{k_x^2}\cos(k_x\chi)dk_x \\ &= \int_0^\infty F_1(k_x)\cdot F_2(k_x)dk_x = \pi\int_{-\infty}^{\infty} f_1(x)\cdot f_2(x)dx \quad \text{(A1)}\end{aligned}$$

Let us define $F_1(k_x) = \sin(k_x\Delta x)/k_x$ and $F_2(k_x) = \sin(k_x\Delta x/2)\cos(k_x\chi)/k_x$. With aid of the formula 3.741.2 [5], $f_1(x)$ can be solved as

$$f_1(x) = \frac{1}{2\pi}\int_{-\infty}^{\infty}\frac{\sin(k_x\Delta x)}{k_x}\cos(k_x x)dk_x = \begin{cases}\frac{1}{4}, & |x| < \Delta x \\ 0, & \text{otherwise}\end{cases} \quad \text{(A2)}$$

Using formula 3.741.3 in [5], $f_2(x)$ can be easily obtained as

$$\begin{aligned}f_2(x) &= \frac{1}{2\pi}\int_{-\infty}^{\infty}\frac{\sin(k_x\frac{\Delta x}{2})}{k_x}\cos(k_x\chi)\cos(k_x x)dk_x \\ &= \frac{1}{4}\mathrm{rect}\Big(\frac{x-\chi}{\Delta x}\Big) + \frac{1}{4}\mathrm{rect}\Big(\frac{x+\chi}{\Delta x}\Big) \quad \text{(A3)}\end{aligned}$$

Substituting eq. (A2) and eq. (A3) into eq. (A1), it can be represented analytically as

$$\begin{aligned}\mathcal{S}_h(\chi) &= \int_0^\infty \frac{\sin(k_x\frac{\Delta x}{2})\sin(k_x\Delta x)}{k_x^2}\cos(k_x\chi)dk_x \\ &= \begin{cases}\frac{\pi}{2}(\frac{\Delta x}{4}), & |\chi| < \frac{\Delta x}{2} \\ \frac{\pi}{2}(\frac{3}{8}\Delta x - \frac{1}{4}|\chi|), & \frac{\Delta x}{2} \le |\chi| < \frac{3\Delta x}{2} \\ 0, & \text{otherwise}\end{cases} \quad \text{(A4)}\end{aligned}$$

REFERENCES

1. Park, S. O., C. A. Balanis, and C. R. Birtcher, "Analytical evaluation of the asymptotic impedance matrix of a grounded dielectric slab with roof-top functions," *IEEE Trans. Microwave Theory Tech.*, Vol. MTT-46, No. 2, 251–259, Feb. 1998.
2. Jackson, R. W. and D. M. Pozar, "Microstrip open-end and gap discontinuities," *IEEE Trans. Microwave Theory Tech.*, Vol. MTT-33, 1036–1042, Oct. 1985.
3. Pozar, D. M., "Input impedance and mutual coupling of rectangular microstrip antennas," *IEEE Trans. Antennas Propagations*, Vol. AP-30, 1191–1196, Nov. 1982.

4. Park, S. O. and C. A. Balanis, "Analytical transform technique to evaluate the asymptotic part of impedance matrix of Sommerfeld-type integrals," *IEEE Trans. Antennas Propagation*, Vol. AP-45, 798–805, May 1997.
5. Gradshteyn, I. S. and I. M. Ryzhik, *Table of Integrals, Series, and Products*, Academic, New York, 1985.
6. Aksun, M. I. and R. Mittra, "Estimations of spurious radiation from microstrip etches using closed-form Green's functions," *IEEE Trans. Microwave Theory Tech.*, Vol. MTT-40, No. 11, 2063–2069, Nov. 1992.
7. Park, I., R. Mittra, and M. I. Aksun, "Numerically efficient analysis of planar microstrip configurations using closed-form Green's functions," *IEEE Trans. Microwave Theory Tech.*, Vol. MTT-43, 394–4000, Feb. 1995.
8. Sarkar, T. K., Z. A. Maricevic, and M. Kahrlzl, "An accurate de-embedding procedure for characterizing discontinuities," *Int. journal of Microwave and Millimeter-Wave Computer-Aided Engineering*, Vol. 2, No. 3, 135–143, 1992.